american physiological society

JNP JOURNAL OF NEUROPHYSIOLOGY

J Neurophysiol 133: 1665–1674, 2025.
First published April 2, 2025; doi:10.1152/jn.00153.2024

RESEARCH ARTICLE

Control of Movement

Spatiomotor dynamics of hand movements during the drawing of memory-guided trajectories without visual feedback

Christopher W. Tyler,[1,2] Kristyo N. Mineff,[1] Michael Liang,[1] and Lora T. Likova[1]

[1]*Smith-Kettlewell Eye Research Institute, San Francisco, California, United States and* [2]*Department of Optometry and Visual Sciences, City St George's, University of London, London, United Kingdom*

Abstract

Although the underlying principles of the spatiomotor dynamics during human movement execution are now broadly understood to conform to a minimum jerk principle, the question addressed in the present analysis is whether different principles operate during human drawing movements without visual input, deriving from studies of the Likova Cognitive-Kinesthetic Memory-Drawing Training. For two groups of participants, completely blind, and sighted but temporarily blindfolded, this analysis shows that the consensus model of arm-motion kinematics as a simple one-third power relationship of drawing speed to the local curvature of the line being drawn is not a sufficient characterization of their coupling. Instead, the drawing dynamics without visual feedback conform to a hyperbolic power relationship, with a coupling power of approximately 1.0 for regions of the highest curvature, asymptoting to curvature-independence for regions of shallow curvature, for both blind and blindfolded groups. Thus, the asymptotic power was much higher than the one-third power predicted by the minimum jerk principle. In detail, the maximum-velocity asymptote for both groups averaged about 6 cm/s for drawing from memory, increasing to more than twice as fast for mindless scribbling. We conclude that the more elaborate operating principle of a hyperbolic saturation function, with a power asymptote of about 1.0, may be interpreted as an adaptive implementation approximating the Minimum Jerk Principle of the simple one-third power law relating velocity and curvature.

NEW & NOTEWORTHY This study reevaluates the one-third power law proposed to govern arm-motion kinematics relating drawing speed to the local curvature of the line being drawn. For complex drawings guided by memory without visual feedback, we find that the relationship is better characterized as a steeper power function that asymptotes to a constant speed for shallow curvatures, empirically approximating the predictions of the minimum jerk principle.

hand movements; manual dexterity; minimum jerk principle; power law; spatiomotor dynamics

INTRODUCTION

The underlying principles of the spatiomotor dynamics during human movement execution, in general, are now broadly understood (1–7). The movement tasks involved in such analyses are typically to reach a defined goal under time and/or accuracy constraints, without specifying what the trajectory of the movement should be. Under these task demands, the trajectory is free to be determined by the agent according to the endpoint criteria (location and time) that combine to define its efficiency. The question addressed in the present analysis, on the other hand, is whether the same principles operate during human nonvisual drawing movements, in which the goal is to match the entire trajectory of an internal memory image to be drawn, as opposed to the unconstrained trajectory in typical goal-oriented movement tasks. An intermediate case is a trajectory constrained by a series of intervening target locations (8, 9). Where the trajectory is constrained, the question is how the agent manages the speed of the trajectory in relation to its form (as defined by its intrinsic curvature), and whether it follows the same or different operational principles as for the execution of unconstrained trajectories.

The study grew out of the Likova Cognitive-Kinesthetic Memory-Drawing training method (10–13), which, for the first time, enabled blind and blindfolded individuals to create complex nonvisual drawings—such as faces and

Correspondence: C. W. Tyler (cwt@ski.org).
Submitted 11 April 2024 / Revised 24 May 2024 / Accepted 29 March 2025

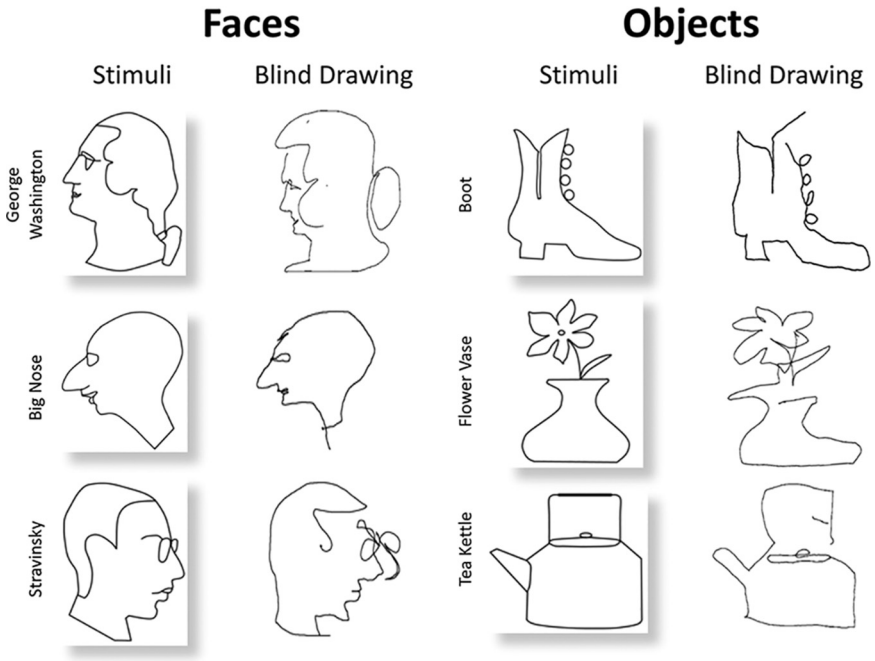

Figure 1. Examples of tactile raised-line stimuli (*left columns*) haptically explored by blind people, and how they were remembered and drawn-from memory without any visual feedback (*right columns*) after the Cognitive-Kinesthetic Training [after Likova (13)].

objects—for recording and analysis (see Fig. 1 for examples). Remarkably, participants were even able to produce these drawings within the confined space of an MRI scanner. The focus on the manual dynamics of producing such drawings, guided solely by memory images, inspired the present analysis of nonvisual drawings in comparison to published studies on the dynamics of visually guided drawing.

A key principle underlying unconstrained human movement trajectories is the maximization of motion smoothness, achieved by minimizing higher-order motion derivatives, such as jerk (3, 8, 14). This principle has been shown to approximate a one-third power law, relating the speed of motion to the curvature of the trajectory[1]. This relationship has also been shown to apply to drawing movements for a continuously defined trajectory (2, 15), and to correspond to moving at a constant equi-affine speed (1, 16–18). It implements the optimization of either kinematic (3, 8, 14) or dynamic (19) criteria of the motion trajectory, corresponding to the minimization of the variance of the movement (20–22). These kinematic constraints were shown to hold both with respect to movement production (15) and perception (23, 24).

The aim of this study was to determine whether the same principles apply to generating movement trajectories without visual feedback, specifically in the context of complex drawings guided by spatial memory. Unlike previous research, our study focused on assessing purely feedforward drawing dynamics by testing blind participants and sighted controls wearing blindfolds to eliminate visual feedback. The main issue addressed by blind drawing is to determine whether adherence to the one-third power law is a function of closed-loop motor control with visual feedback, or is applicable to the open-loop condition of drawing from memory with no feedback as to the adherence of the trajectory to a visual template. Of course, the memory-drawing case is still guided by kinesthetic feedback as to whether the output motor commands are providing the intended movement, but it is open-loop with respect to any external criterion of the trajectory to be followed.

A second issue is to which law the motions are expected to conform. The original proposal was the isogony principle of Viviani and Terzuolo (25), that the drawing speed would conform to a constant angular velocity for any circular arc, meaning that the angular velocity should be directly proportional to the local radius of curvature of any arbitrary curve. It is somewhat curious that Lacquaniti et al. (2) elaborated this principle to the concept of a nonunitary power function of the radius of curvature, which translates to a roughly one-third power function prediction of the radius of curvature. Thus, this prediction is a long way from the linear proportionality of the isogony principle but conforms approximately to the one-third power predicted from the minimum jerk principle described above. Moreover, the minimum jerk principle does not predict a constant velocity along circular arcs of different lengths, as would the isogony principle. Instead, it predicts a smooth acceleration to the center of the arc and deceleration from it according to the principle of minimizing the second derivative of velocity, or jerk (15), as in the operation of smooth elevator trajectories in the engineering domain.

However, the empirical power fits in most studies vary around the one-third value, both across the average speed of the drawn trajectory (2) and with the complexity of the drawing (5, 26). There is a possibility that this variation in power exponents is related to the presence of visual feedback of the accuracy of adherence to the designated trajectory, which can be tested by performing the drawing under visually open-loop conditions (i.e., with eyes closed). The present

[1]This law is also often expressed as a two-thirds power law of angular speed ω to curvature κ, where the angular speed is a function of the radius of curvature. We have preferred to express it in terms of Lagrangian (local) speed along the curved trajectory, when it becomes a one-third power law of the radius of curvature.

study thus provides this test, both in unpracticed sighted individuals when the visual feedback loop is opened by closing the eyes, and in the well-practiced condition of blind individuals with many years' experience of operating without visual feedback.

Hypotheses

1) The primary hypothesis for the speed/curvature relationship is that it should conform to the one-third power law propounded by Lacquiniti et al. (2), Flash and Hogan (3), and Polyakov et al. (4, 27), when expressed in terms of radius of curvature.
2) The secondary hypothesis for this function is that it may be an intermediate segment of a hyperbolic saturation function in which the power-law exponent asymptotes to 1 at small radii of curvature and to zero for large radii of curvature.
3) The tertiary hypothesis is that the hyperbolic power should conform to the version of the minimum jerk principle developed by Huh and Sejnowski (26), according to which the exponent decreases with the angular frequency of the drawing oscillations, from a value of about two-thirds for angular frequencies < 1, asymptoting toward zero for high ones.

MATERIALS AND METHODS

Participants

The participants in the study were 12 blind and 4 normally sighted individuals, as tabulated in Table 1. The study was approved by the Smith–Kettlewell Institutional Review Board and is in conformity with the Helsinki Declaration.

Procedures

The data for this analysis come from a unique study in which through the Cognitive–Kinesthetic Drawing Training method, developed by Likova (see Refs. 10–13, 28, 29), blind individuals and blindfolded sighted controls are trained to draw from memory, learning in the process and encoding in memory the configurations of different complex spatial structures, such as faces and objects, as in the examples shown in Fig. 1.

As described in these studies, the Cognitive-Kinesthetic training itself is an implicit form of active learning. It involves a complex interactive process practiced with various images of both objects and faces. Participants received instruction on how to "see" the configuration of a raised-line drawing using one hand, as opposed to the habitual two-handed approach typical in blind shape acquisition. They also learned how to hold a drawing stylus and replicate the drawing from spatial memory with the other hand. The separate-hand transfer method was specifically designed to enhance spatial memory representation of the image to be drawn, rather than reinforcing "muscle" memory of tactile exploration movements. This distinction is particularly relevant, as using the same hand for both perception/memorization and memory-guided drawing might otherwise lead to a reliance on muscle memory rather than true spatial encoding. Informal feedback from participants validated the empowerment they received through this approach. Many remarked that this Cognitive-Kinesthetic drawing training significantly enhanced their sense of spatial layout and everyday functioning, and even had a positive impact on their spatial navigation skills.

The Cognitive-Kinesthetic Drawing Training was keyed to an fMRI protocol in which each drawing had to be completed within a 20 s time period with no visual feedback. After the training, all participants were thus relatively proficient in rapidly drawing images from memory even in the scanner. Those blind participants with residual vision were blindfolded to ensure that no visual information was accessible during the drawing procedures. For this study, the drawing movements were tracked both spatially and temporally with an MR-compatible tablet, allowing various aspects of the

Table 1. *Participant demographics*

Condition	Age, yr	Gender	Current Visual Status	Age of Onset	Visual Status at Birth	Diagnosis	Braille Fluency	Age-Onset, yr	Years of Full Vision
Trained with serious visual impairment	68	0	NLP	15	LP	Retinopathy of prematurity	4	53	15
	66	1	LP	<1	LP	Retinopathy of prematurity	4	66	0
	57	1	LP	30	Tunnel vision	Retinitis pigmentosa	4	27	30
	76	0	LP	16	Full vision	Optic neuropathy	3	60	16
	31	1	NLP	28	LP	Optic nerve hypoplasia	4	3	0
	66	1	NLP	16	Full vision	Glaucoma	3	21	16
	37	1	HM	<1	HM	Congenital optic neuropathy	4	37	0
	56	0	LP	47	Full vision	Glaucoma	0	9	47
	37	0	LV	30	Full vision	Optic nerve damage	1	7	30
	75	1	LV	64	Full vision	Cataract/Macular degeneration	0	11	64
	27	1	NLP	<1	LP	Retinopathy of prematurity	4	27	0
	47	0	LP	8	LP	Brain tumor to optic nerve	4	39	8
Average	53.58	5M/7F		28.22			2.92	30	18.83
SD	17.33			17.75			1.62	21.35	20.56
Blindfolded	60	0	N	0	Full vision	None	0	60	60
	59	1	N	0	Full vision	None	0	59	59
	31	1	N	0	Full vision	None	0	31	31
	26	0	N	0	Full vision	None	0	26	26
Average	44	2M/2F					0	44	44
SD	18.02							18.02	18.02

F, female; HM, high myopia; LP, light perception only; LV, low vision; M, male; NLP, no light perception; SD, standard deviation.

drawing dynamics to be analyzed quantitatively. The drawing analyses are shown in Fig. 2, as follows:

1) Spatiotemporal drawing trajectory, plotting x, y position throughout the trajectory with instantaneous speed (i.e., coordinate-free, or Lagrangian, velocity) indicated by the color as coded in the color bar. Each trajectory had a duration of 20 s and was sampled at a spatial resolution of 0.25 cm, providing of the order of 200–600 samples per trajectory.
2) Plot of the instantaneous speed as a function of local radius of curvature at each point along the trajectory. The two curves are fits of a model derived from a hyperbolic power-law analysis of this relationship, where the fit for small radii of curvature is controlled by a power function leveling off to a constant velocity for large radii of curvature. The data are fit separately for the first and second halves of the trajectory. In this case, the asymptotic power, q, for small radii or curvature was ~1 and the asymptotic maximum velocity, v_{Max}, was ~6 cm/s.
3) Plot of the absolute instantaneous speed as a function of length along the trajectory, with the same color coding as for A. Velocities ranged from about 1–50 cm/s.
4) Log plot of the local radius of curvature as a function of length along the trajectory. Radii of curvature ranged from about 0.5–40 cm.

Method for Processing and Cleaning the Drawing Dynamic Analyses

Since the drawing tasks were completed while inside the MRI scanner with an fMRI-compatible drawing lectern over the abdomen, participants may have experienced some unnatural restriction in movement due to the limited space of the bore aperture adjacent to the drawing surface. Such spurious contacts would register as an extremely high-velocity drawing segment, which we refer to as a "glitch" that meets the criteria to be removed from the drawing. To clean and process such glitches in the drawings, a "glitchThresh" function was implemented in the speed curvature model analyses to remove the segments in the drawing where the spurious segments occurred. The glitchThresh function removed any change in distance larger than this input value in the (x, y) coordinate system of the tablet from the first point of contact (the stylus) to the second point of contact (some part of the drawing hand).

Table 2 details the average glitch thresholds (± 1 standard deviation) of the (x, y) distance in mm, and the numbers and proportions of the drawings that needed to be cleaned in each drawing condition from one or more glitches occurring during the period of each of the tasks in the study: Draw from Memory (two repeats: DM1 and DM2) or Draw Scribble (DS1 and DS2) between the blind and blindfolded groups. The DS

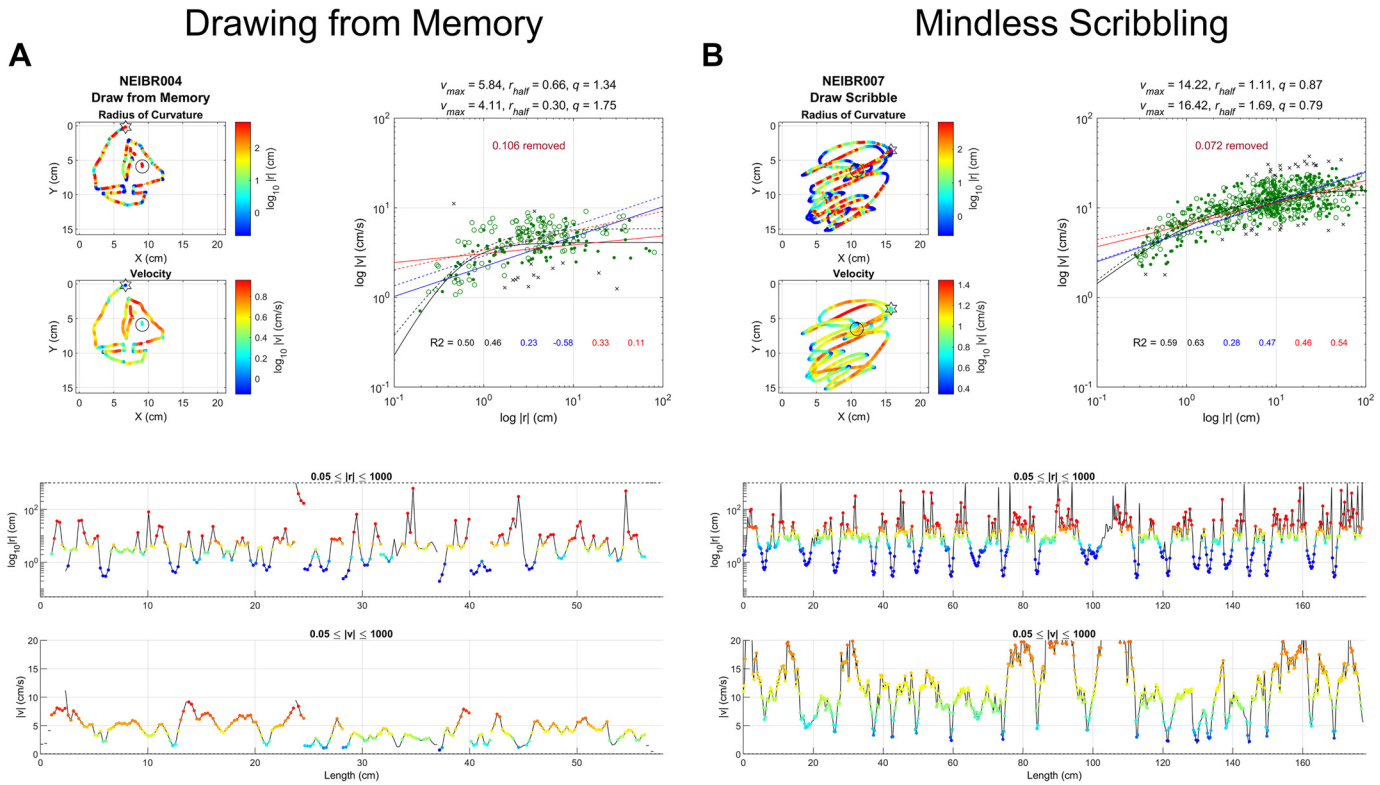

Figure 2. Plots of the analysis variables for example drawing (*A*) and scribbling (*B*) trajectories. Upper left quadrant: (x, y) plots of the drawing trajectory color coded according to instantaneous velocity (*top plot*) and curvature (*bottom plot*). *Bottom half*: Plots of the velocity (*top plot*) and curvature (*bottom plot*) as a function of distance along the trajectory, color coded according to the respective parameter value. *Top right quadrant*: Scatterplot of log velocity vs. log radius of curvature for the first half (open circles) and the second half (filled circles) of each drawing trajectory. Pairs of solid curves are the fits of the one-third power law (blue), variable power function (red), and hyperbolic saturation (black) models to each half of the datasets. Note that the data fall consistently below either power law at both extremes of radii of curvature, supporting the need for the hyperbolic saturation analysis.

J Neurophysiol • doi:10.1152/jn.00153.2024 • www.jn.org

tasks had the lowest proportion of drawings requiring cleaning since subjects were instructed to keep the stylus down for the entire task, reducing the need to adjust hand placement when holding the stylus. Many drawing epochs had more than one double-contact glitch. In the blind group, the proportion of DM1 and DM2 drawings requiring cleaning with the glitchThresh approach were 63% and 63% for the blind group, and 83% and 61%, respectively, for the blindfolded group. DS1 and DS2 drawings needed similar or less cleaning, 63% and 44% in the blind and 38% and 38% in the blindfolded group, respectively. Between the two groups, a total of 102 drawings per drawing condition sequence, 79 drawings per condition in the blind group and 23 drawings per condition in the blindfolded group, were recorded and the proportion of drawings that were cleaned is given in Table 2. Thus, the proportion of drawings that required cleaning was much higher for the DM than for the DS conditions, due to the difference in operating instructions for the two tasks.

However, the cleaning had little effect on the mean values reported in this paper. Its main effect was to remove outliers from the distributions plotted in RESULTS, thus permitting a more discriminative analysis of the model fitting parameters. Examples of the outliers removed from the instantaneous velocity analysis may be seen as the *X*s in Fig. 2*A* and *B*, making it clear that the cleaned points form a noisy penumbra well outside the main cloud of the true drawing points. The result of the cleaning procedure was a total of 188 drawings by the blind group and 52 drawings by the blindfolded group.

Theoretical Analysis

Inspection of the speed/curvature data shows that there is a strong relationship between drawing speed and the local curvature of the drawing trajectory, similar to the results of Lacquaniti et al. (2), Flash and Hogan (3), and Polyakov et al. (4, 27). However, it was evident that many datasets exhibited a deviation from a uniform power relationship (straight line in log-log coordinates), leveling off at a constant saturation level for some range of the largest radii of curvature. The data were, therefore, fit with a hyperbolic saturation function of the form:

$$\text{Speed} = v_{Max}/(1 + r_{Half}/r^{q}), \quad (1)$$

where r is the radius of curvature, v_{Max} is the asymptotic limit at large radii of curvature, *rHalf* is the transition between the two hyperbolic asymptotes, and q is the exponent of the asymptote for small radii of curvature. A similar function was introduced by Viviani and Stucchi (23) and Viviani and Flash (15), based on an analysis in Viviani and Schneider (30). Their equation was:

$$V = v_1\left(r/(1 + \alpha r)\right)^{q}, \quad (2)$$

which has a softer approach to the asymptotes for high q values than our formulation. The Viviani and Stucchi (23) paper evaluated the empirical fit of one parametrization of their function to a large set of freehand scribbling data by the laborious procedure of dividing each trace into segments defined by the successive inflection points in the scribbled trajectory and fitting the hyperbolic saturation function separately to each segment. The details are obscure, but they report that the best-fitting exponent derived from this procedure was almost exactly one-third.

The analysis proceeded according to a nested model structure based on *Eq. 1*. The next simpler model is the two-parameter power model:

$$\text{Speed} = v_1/r^{q}, \quad (3)$$

where v_1 is the scaling parameter corresponding to v_{Max} in *Eq. 1* with the exponent q free to vary when applied to the present complex drawing motions. The one-parameter version of this model is the fixed power function:

$$\text{Speed} = v_1/r^{1/3}, \quad (4)$$

and q is set to the typical value reported in previous studies, which has been consistently reported to be 0.33 across a broad range of motor tasks (see INTRODUCTION).

Thus, the first analysis is to compare the power function fits with the fixed power of $q = 1/3$ (*Eq. 4*) against the unconstrained power law (*Eq. 3*). The next level of the procedure is then to compare that unconstrained power law with the hyperbolic power law of *Eq. 1*, which captures the degree to which the power is uniformly distributed over degrees of curvature, as opposed to being the transition between two asymptotes, with a steeper power limb and a constant maximum speed. For direct comparison with the previous literature, it is also of interest to compare the fixed power law with the hyperbolic saturation power function.

RESULTS

The analysis provides average results of the drawing dynamics analysis for both the blind and blindfolded sighted participants for the speed/curvature fits of the hyperbolic saturation function (3 parameters) and its nested subcases, the power-law fit (2 parameters) and the one-third power fit (1 parameter). The results were initially tabulated separately for each repeat of the drawing sequence (DM1 and DM2; DS1 and DS2), but none of the parameters were not significantly different for the repeat conditions, so the two repeats for each type of drawing were combined for the averaged analysis of Tables 3, 4 and 5.

Table 3 compares the accuracy of the fits of the three nested models to the speed/curvature data averaged for the DM and DS conditions, separately for the whole and the first

Table 2. *Statistics of glitch threshold values used to clean images across each drawing condition*

	Blind				Blindfolded			
	DM1	DM2	DS1	DS2	DM1	DM2	DS1	DS2
Average glitchThresh ± SD, mm	11.1 ± 19.9	8.5 ± 14	21.3 ± 16.1	32.1 ± 5.2	6.2 ± 10.5	4.1 ± 2.2	8.8 ± 7.8	11.1 ± 16.5
Number drawings cleaned	51	50	51	36	20	14	9	9
Total drawings	81	79	81	81	24	23	24	24
Proportions cleaned	63%	63%	63%	44%	83%	61%	38%	38%

DM, drawing from memory; DS, draw scribble; SD, standard deviation.

and second halves of each 20 s drawing epoch (the parameter values of the fits are provided in the subsequent tables, Tables 4 and 5). The fits are assessed in terms of the "average residual variance" for each of the three models fitted to the individual data for the blind group. Each fit uses over 200 speed/curvature points for the full condition, or over 100 points for each half condition. (Note that the variance accounted can go below zero if the model parameters are such that the deviations of the points from the fitted function are greater than their deviation from the null hypothesis of their own mean value, making the residual variance > 1. This behavior can occur for models with fixed parameters, such as the one-third power law.) The significance levels are chosen to correct for 100 applications of the statistical tests by the Bonferroni criterion, with the three significance codes corresponding to corrected levels of $P < 0.05$, 0.01, and 0.001, respectively, after accounting for the one and two extra free parameters in the variable power and hyperbolic saturation models. The significance levels, shown by the 1-, 2-, and 3-asterisk code in the righthand columns of Table 3, are taken as $t(160)$ >3.6 ($P < 0.05$), >4.0 ($P < 0.01$), and >4.6 ($P < 0.001$), respectively, for the three significance levels for the blind group, and $t(47)$ >3.7 ($P < 0.05$), >4.2 ($P < 0.01$), and >4.8 ($P < 0.001$), respectively, for the blindfolded group.

The results in Table 3 show quite similar model-fit variances throughout the first and second half-periods. For both the blind groups the hyperbolic saturation function fitted significantly better than the fixed one-third power law for both DM and DS, though not significantly better than the variable-exponent fit. In turn, the variable-exponent power law fitted significantly better than the fixed one-third power law fit for the blind, though only at the uncorrected level for DS. For the blindfolded, both the hyperbolic saturation function and the variable-exponent functions fitted significantly better than the fixed one-third power law for DS, though not for DM. The overall picture is therefore that the hyperbolic saturation model provides a much better fit to both datasets than the simple one-third power law, with partially significant differences in favor of the variable-exponent over the fixed one-third power law model.

Table 4 shows the average parameter values of the drawing dynamics analysis for the blind participants for the individual speed/curvature fits of the hyperbolic saturation function (3 parameters) and their nested subcases, the power-law regression (2 parameters), and the one-third power fit (1 parameter). As was the case for the residual variances, many of the parameters of the fits were not significantly different for the repeat conditions (DM1 and DM2; DS1 and DS2), so they were combined for the averaged analysis of parameter values in Tables 4 and 5. These average parameter values were significantly different between the blind and blindfolded groups, and also between the two types of drawing motion, DM and DS, at high significance for the blind group conditions, Table 4 (though not for this comparison in the smaller blindfolded group, Table 5). The significant parameter-value comparisons will therefore be detailed in the following paragraphs.

The parameters of the model fit are provided for the blind group in Table 4. The parameters are the asymptotic maximum velocity for the hyperbolic model, or velocity at a radius of 1 cm for the power law models (v_{Max} or v_1 in deg/s), the radius of curvature at the half-maximum velocity (r_{Half} in cm), and the dimensionless exponent (q) of the power function models or its asymptote for small radii of curvature for the hyperbolic saturation model.

The best-fitting parameter values for the three model fits for the Blind group are shown in the left section of Table 4, with the means ± its standard error (SEM) below them. The significance coding in Table 4 is shown in the columns to the right of the parameter values for the DM versus DS comparisons, and below and to the right for the comparisons between the three nested model types. The significance levels, shown by the asterisk code in the upper righthand columns, are taken as $t(160)$ >3.6 ($P < 0.05$), >4.1 ($P < 0.01$), and >4.7 ($P < 0.001$) for the three significance levels for the blind group, and $t(47)$ >4.5 ($P < 0.05$), >4.8 ($P < 0.01$), and >5.3 ($P < 0.001$) for the blindfolded group, with Bonferroni correction for 100 applications of the statistical tests.

The key question targeted in this paper is the model structure that best describes the nonvisual drawing behavior, which is addressed in the lower right sections of Tables 4 and 5. Of particular interest is the value of q for the present paradigm, which is the key parameter in common between the three models. If the Lacquaniti et al. (2) model is applied to the present drawing data for the blind group, q would take

Table 3. *Average variance accounted for and comparative significance of nested models*

Blind	*n* = 160	*n* = 162			Blindfolded	*n* = 47	*n* = 48		
Condition	DM	DS	Significance		Condition	DM	DS	Significance	
Model type			Hyp vs. Var		Model Type			Hyp vs. Var	
Hyperbolic full	0.31	0.41	ns	ns	Hyperbolic Full	0.34	0.37	ns	ns
1st half	0.28	0.44	ns	ns	1st half	0.33	0.39	ns	ns
2nd half	0.33	0.41	ns	ns	2nd half	0.39	0.38	ns	ns
			Hyp vs. 1/3 power					Hyp vs. 1/3 power	
Variable exponent	0.00	0.31	***	***	Variable Exponent	0.22	0.23	ns	***
1st half	0.21	0.32	***	***	1st half	0.22	0.24	ns	***
2nd half	0.22	0.30	***	***	2nd half	0.24	0.23	*	***
			Var vs. 1/3 power					Var vs. 1/3 power	
1/3 Power law	−0.13	0.08	**	*	1/3 Power Law	0.00	−0.41	ns	**
1st half	−0.29	0.09	***	*	1st half	−0.10	−0.48	ns	**
2nd half	−0.22	0.03	***	**	2nd half	0.01	−0.39	ns	***

Average proportions of residual variance of the speed/curvature relationships accounted for by each of the three nested models in the MemoryDraw (DM) and Scribble (DS) conditions, with their comparative statistical significances, for the blind and blindfolded groups. DM, drawing from memory; DS, draw scribble; *n*, number of drawings. Significance code: *< 0.05; **< 0.01; ***< 0.001 (Bonferroni corrected for 100 test applications).

Table 4. *Parameter values and their significances for the model fits for the blind group*

Blind Group							Significances		
Condition		DM			DS		t(DM − DS)		
Model type	vMax/v1	q	rHalf	vMax/v1	q	rHalf	vMax/v1	q	rHalf
Hyperbolic full	6.763	0.876	0.536	19.480	0.949	0.765	***	ns	ns
Variable exponent	3.859	0.157		10.519	0.175		***	ns	
1/3 Power law	3.403	0.333		8.653	0.333		***		
							DM	DS	
Means ± SEM							Hyperbolic vs. variable q		
Hyperbolic full	0.384	0.065	0.069	1.307	0.037	0.075	***	***	
Variable exponent	0.173	0.011		0.511	0.009		Hyperbolic q vs. 1/3		
1/3 Power law	0.147	0.333		0.417	0.333		***	***	
							Variable q vs. 1/3		
							***	***	

Average parameter values of the speed/curvature relationships accounted for by each of the three nested models in the DM and DS conditions, with their comparative statistical significances, for the blind group. The first column for each condition is for v_{Max} in cm /s for the full hyperbolic model followed by the v intercepts at 1 cm/s for the other two models and the intersection radius of the two hyperbolic asymptotes in centimeters. DM, drawing from memory; DS, draw scribble. Significance code: *< 0.05; **< 0.01; ***< 0.001 (Bonferroni corrected for 100 test applications).

the value of 0.33 and r_{Half} would be larger than the largest value in the range of the data analysis, which was 40 cm, resulting in a pure one-third power function. For the blind group (Table 4), the average values of exponent q for the hyperbolic and the variable-exponent models fitted to the DM data, at $q = 0.88$ and 0.16, respectively, are both highly significantly different from the theoretical value of 0.33 (and from each other). The ratios are similar for DS, at $q = 0.95$ and 0.18, respectively, again all different from each other to high significance. Similar relationships were obtained for the drawing parameters of blindfolded group (Table 5), with q ratios 1.15 and 0.17, respectively, for DM and 1.06 and 0.14, respectively, for DS. These values are again all mutually different at the high significance level for DM and at marginal to high levels for DS. In particular, these comparisons make clear that the exponent in the regions of small radius of curvature is much higher, with a value of ~1.0 than the theoretical prediction of 0.33.

The steeper q for the hyperbolic saturation model fits is consistent with the shallower q for the variable-exponent model fits because the zero slope of the maximum velocity saturation asymptote, v_{Max} makes the overall function shallower than the one-third slope over most of the fitted range. It is only for the range of small radii of curvature that the steeper slope is expressed. The hyperbolic fits showed a highly significant difference between the maximum velocity, v_{Max} for the DM task, at 6.76 ± 0.38 cm/s, and the DS tasks, at nearly triple the velocity of 19.48 ± 1.31 cm/s (upper right-hand panel of Table 4). Corresponding significant differences are seen for the equivalent v_1 parameter for the variable- and fixed-exponent models.

The final comparison is of the fitted parameter values for the blind and blindfolded groups. None of the differences between groups are significant at the corrected criterion level. Thus, the differences between DM and DS for the three sets of model parameters described in Tables 4 and 5 are generally similar for the two groups.

These characteristics are illustrated in the further examples of Fig. 3, showing the pronounced saturation of the drawing velocity at large radii of curvature and the pronounced steepening of the exponent to values much greater than one-third at the smallest radii of curvature. Note also that the distance functions of the speed, |v|, and radius of curvature, |r|, plotted in the lower halves of the figures make

Table 5. *Parameter values and their significances for the model fits for the blindfolded group*

Blindfolded group							Significances		
Condition		DM			DS		t(DM − DS)		
Model type	vMax/v1	q	rHalf	vMax/v1	q	rHalf	vMax/v1	q	rHalf
Hyperbolic full	6.049	1.148	0.392	13.693	1.062	0.560	*	ns	ns
Variable exponent	3.762	0.173		8.577	0.144		*	ns	
1/3 Power law	3.359	0.333		7.524	0.333		**		
							DM	DS	
Means ± SEM							Hyperbolic vs. variable q		
Hyperbolic Full	0.542	0.135	0.087	1.928	0.208	0.114	***	**	
Variable Exponent	0.270	0.023		1.261	0.017		Hyperbolic q vs. 1/3		
1/3 Power Law	0.234	0.333		1.004	0.333		***	*	
							Variable q vs. 1/3		
							***	***	

Average parameter values of the speed/curvature relationships accounted for by each of the three nested models in the DM and DS conditions for the blindfolded group. The first column for each condition is for v_{Max} in cm/s for the full hyperbolic model followed by the v intercepts at 1 cm/s for the other two models and the intersection radius of the two hyperbolic asymptotes in centimeters. DM, drawing from memory; DS, draw scribble. Significance code: *< 0.05; **< 0.01; ***< 0.001 (Bonferroni corrected for 100 test applications).

the result that, although some minima of the two distance functions do coincide, many do not, making it difficult to perform the piece-wise analysis of Edelman and Flash (31) and Polyakov (4, 27), for the functions between corresponding pairs of minima, on the present data. The same issue was addressed by Richardson and Flash (9).

DISCUSSION

The main goal of the paper was to evaluate the kinematic processes of drawing complex line-images from memory and to do so in relation to the general kinematic principles of arm movement control developed by Viviani, Hogan, Flash, and colleagues (1, 3, 5, 14, 15, 17, 18, 24, 25, 32), among many others. The consistent principle found in these studies approximated a one-third power law for the relationship between the speed of the trajectory and its curvature. A subset of such studies have assessed the application of this principle to controlled drawing movements, and have done so have used relatively simple drawings with little demand on memory (2, 5, 9, 15, 23, 26, 33, 34). Thus, it remained an open question how this principle would apply to the kinematics of complex drawings with high memory demand. Our study of such performance also differed from the others in assessing drawing without visual feedback, by testing blind participants and sighted controls with blindfolds to eliminate the visual feedback of typical studies of visually guided arm movements.

The present nonvisual drawing data provide general support for the speed/curvature power law, though in a more complex form than the simple one-third power law. Inspection of the data suggested that speed asymptoted to a constant value at large radii of curvature (shallow curvatures), so they were fit with a "hyperbolic saturation function" of a power law for small radii of curvature with an asymptotic speed limit for large radii of curvature. This function, similar to the one that had been introduced by Viviani and Stucchi (23, their *Eq. 1*), gave a significantly better fit to our data in many cases than the simple one-third power law (Table 3). The rising portion of the curvature range of the fits extended only up to radii of ~1 cm, with powers of about triple the one-third value in the rising portion of the function, whereas if the simple power law prediction held, this hyperbolic model fit would cover the entire range up to the maximal assessed radius of 40 cm. These fits, therefore, strongly support the concept of the hyperbolic saturation specification of the speed/curvature relationship, and are consistent with the idea that the initial rising portion has a power of ~1.0, as in the further examples in Fig. 3.

The range of hyperbolic power-law slopes of 0.88–1.15 in the present study (Tables 4 and 5) may be compared with those found by Zago et al. (5) for fits of the unconstrained power law over the full range of radii of curvature, which ranged from ~0.7 for simple figures to ~0.15 for complex figures. Unlike the hyperbolic saturation function, the unconstrained power law fits for the present drawing trajectories, which would be classed as complex figures by the analysis of Zago et al. (5), have powers of the order of 0.15 under all conditions, consistent with the shallow fits to their complex figure data. However, this shallow slope is shown here to be the result of an asymptote to zero slope for large radii of curvature and a markedly steeper slope for the smaller range. It is only when the hyperbolic saturation fits allows the separate assessment of the low and high ranges of radius of curvature that the high powers of ~1.0 become apparent.

In relation to its theoretical roots, we note that the derivation of the power law behavior from the minimum jerk principle (3, 15, 31) was based on the artificial segmentation of the drawing trajectory into individual arcs, and is difficult to apply in general to the kinds of complex drawing used in the present study (Fig. 3, *bottom panels*). For the scribbling task illustrated in Fig. 2 (*right panel*), the minima of the velocity function along the trajectory consistently coincide with those the curvature function, supporting the minimum jerk principle for this primarily motor control task (23, 25). In fact, a lack of such correspondence is far more common for the complex drawing trajectories (Figs. 2 and 3, *bottom panels*), indicating that other principles are at work. We propose that these principles involve details of the retrieval of segments of the complex drawings from memory. However, we do not have access

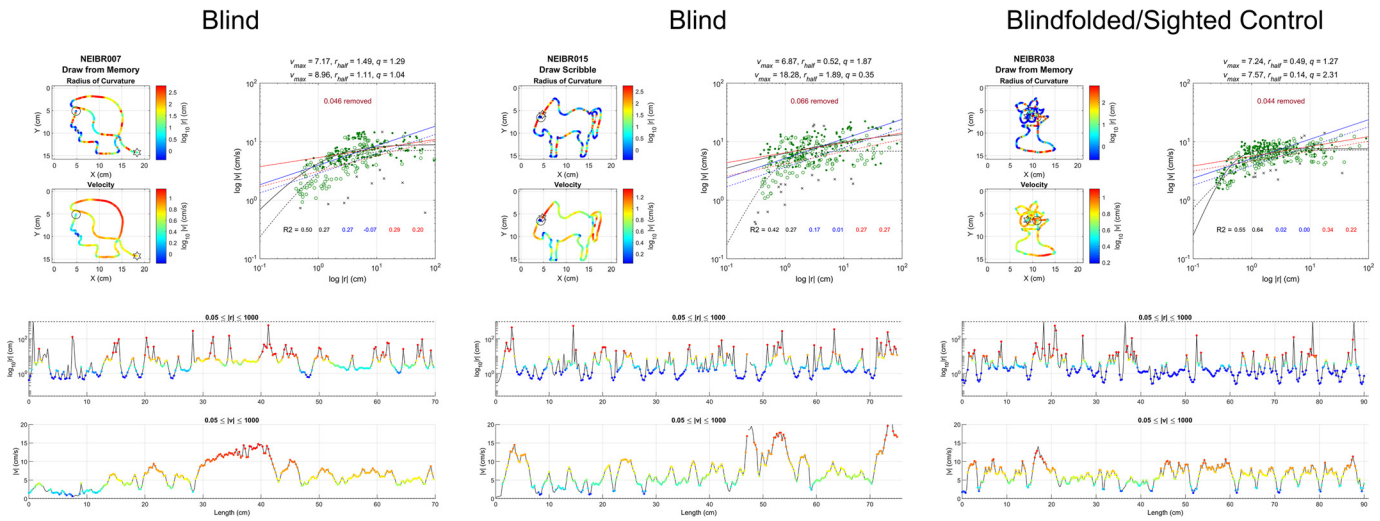

Figure 3. Further examples of a freehand drawing trajectory analysis in the same format as Fig. 2. showing the pronounced flattening from the one-third power law prediction (blue lines in the upper right panels) for large radii of curvature, and steeper rising slopes for small radii of curvature.

to the elements of the memorial segmentation beyond what might be suggested by the curvature function, so a formal test of this hypothesis is not available.

An alternative view on the minimum jerk principle was provided by Huh and Sejnowski (26), whose derivation predicted a power law decreasing with the dimensionless angular frequency of the drawing motion (*Hypothesis 3*), from a value of $\sim$ two-thirds for the lowest angular frequencies, asymptoting down toward zero for angular frequencies of 10 oscillations per unit cycle (i.e., per 2π radians). This result was accurately replicated by Zago et al. (5), though with a different parametrization of the exponent specification. Thus, those results could be said to be consistent with the asymptotic saturation function (*Hypothesis 2*) that gives the best fit to our results.

A key question in this study was whether the task of the feedforward drawing of complex images from memory, as opposed to mindless scribbling movements, makes any difference to the kinematics of the drawing movements. The answer to this question is "yes," since the maximum velocity for the MemoryDraw condition was about one-third of the value for Scribble condition. Thus, in overview, scribbling adheres to the same underlying hyperbolic saturation principle of kinematics, except for the difference in parameter values, although it is a much freer motion than drawing from memory.

Conclusions

In summary, by capitalizing on the Likova Cognitive-Kinesthetic Drawing Training method, we were able to produce, record, and analyze for the first time the nonvisual spatiomotor dynamics of complex drawings, by both blind and blindfolded people. This kinetic analysis sheds light on the validity of the classic minimum jerk model of arm-motion kinematics to the case of memory drawing without visual feedback. In this case, it shows that the simple one-third power relationship of drawing speed to the local curvature of the line being drawn is not a sufficient characterization of the coupling behavior. Instead, the present analysis reveals the operation of a hyperbolic power-law relationship, with the power-law coupling for regions of high curvature, asymptoting to curvature-independence for regions of shallow curvature. After accounting for the saturation region, the power law relating velocity and curvature is found to exhibit a power asymptote of $\sim$1.0, suggesting that the empirical approximation to the minimum jerk principle is adventitiously implemented by the velocity saturation mechanism.

DATA AVAILABILITY

Data processing and analysis may be found at OSF: https://doi.org/10.17605/OSF.IO/PF9HG.

SUPPLEMENTAL MATERIAL

Individual analysis figures may be found at the OSF link https://doi.org/10.17605/OSF.IO/PF9HG.

ACKNOWLEDGMENTS

The authors thank Adam Manoogian for the initial data processing and analysis.

GRANTS

The work is supported by NIH/National Eye Institute EY024056 and National Science Foundation SL-CN1640914 to L. Likova.

DISCLAIMERS

Such as for Government agency work.

DISCLOSURES

No conflicts of interest, financial or otherwise, are declared by the authors.

AUTHOR CONTRIBUTIONS

L.T.L. conceived and designed research; L.T.L. and K.M.N. performed experiments; C.W.T., K.M.N., and M.L. analyzed data; C.W.T., K.N.M., M.L., and L.T.L. interpreted results of experiments; C.W.T. and M.L. drafted manuscript; C.W.T. and M.L. prepared figures; C.W.T., M.L., and L.T.L. edited and revised manuscript; L.T.L. and C.W.T. approved final version of manuscript.

REFERENCES

1. **Viviani P**, **Terzuolo C.** Trajectory determines movement dynamics. *Neurosci* 7: 431–437, 1982. doi:10.1016/0306-4522(82)90277-9.
2. **Lacquaniti F**, **Terzuolo C**, **Viviani P.** The law relating the kinematic and figural aspects of drawing movements. *Acta Psychol (Amst)* 54: 115–130, 1983. doi:10.1016/0001-6918(83)90027-6.
3. **Flash T**, **Hogan N.** The coordination of arm movements: an experimentally confirmed mathematical model. *J Neurosci* 5: 1688–1703, 1985. doi:10.1523/JNEUROSCI.05-07-01688.1985.
4. **Polyakov F**, **Drori R**, **Ben-Shaul Y**, **Abeles M**, **Flash T.** A compact representation of drawing movements with sequences of parabolic primitives. *PLoS Comput Biol* 5: e1000427, 2009. doi:10.1371/journal.pcbi.1000427.
5. **Zago M**, **Matic A**, **Flash T**, **Gomez-Marin A**, **Lacquaniti F.** The speed-curvature power law of movements: a reappraisal. *Exp Brain Res* 236: 69–82, 2018. doi:10.1007/s00221-017-5108-z.
6. **Taylor MM.** Comments on Marken and Shaffer: the power law of movement: an example of a behavioral illusion. *Exp Brain Res* 236: 1531–1535, 2018. doi:10.1007/s00221-018-5192-8.
7. **Flash T.** Brain representations of motion generation and perception: space-time geometries and the arts. In: *Space-Time Geometries for Motion and Perception in the Brain and the Arts*, edited by Flash T, Berthoz A**.** Springer, 2021, p. 3–34.
8. **Todorov E**, **Jordan MI.** Smoothness maximization along a predefined path accurately predicts the speed profiles of complex arm movements. *J Neurophysiol* 80: 696–714, 1998. doi:10.1152/jn.1998.80.2.696.
9. **Richardson MJ**, **Flash T.** Comparing smooth arm movements with the two-thirds power law and the related segmented-control hypothesis. *J Neurosci* 22: 8201–8211, 2002. doi:10.1523/JNEUROSCI.22-18-08201.2002.
10. **Likova LT.** Drawing enhances cross-modal memory plasticity in the human brain: a case study in a totally blind adult. *Front Human Neurosci* 6: 44, 2012. doi:10.3389/fnhum.00044.
11. **Likova LT.** The spatiotopic 'visual' cortex of the blind. *Human Vision Electron Imag* 82910L, 2012. doi:10.1117/12.912257.
12. **Likova LT.** Brain reorganization in adulthood underlying a rapid switch in handedness induced by training in memory-guided drawing. In: *Neuroplasticity*, edited by Chaban V**.** IntechOpen, 2018.
13. **Likova LT.** Harnessing the power of "visual" art: memory-guided drawing training drives rapid neuroplasticity in the blind and sighted. *Optica Society Clinical Vision Sciences Technical Group Webinar*, Mar 9, 2023.
14. **Hogan N.** An organizing principle for a class of voluntary movements. *J Neurosci* 4: 2745–2754, 1984. doi:10.1523/JNEUROSCI.04-11-02745.1984.
15. **Viviani P**, **Flash T.** Minimum-jerk, two-thirds power law, and isochrony: converging approaches to movement planning. *J Exp*

Psychol Hum Percept Perform 21: 32–53, 1995. doi:10.1037//0096-1523.21.1.32.

16. **Pollick FE**, **Sapiro G.** Constant affine velocity predicts the 1/3 power law of planar motion perception and generation. *Vision Res* 37: 347–353, 1997. doi:10.1016/s0042-6989(96)00116-2.
17. **Handzel A**, **Flash T.** Geometric methods in the study of human motor control. *Cog Stud Bull Jap Cogn Sci Soc* 6: 309–321, 1999.
18. **Flash T**, **Handzel AA.** Affine differential geometry analysis of human arm movements. *Biol Cybern* 96: 577–601, 2007. doi:10.1007/s00422-007-0145-5.
19. **Uno Y**, **Kawato M**, **Suzuki R.** Formation and control of optimal trajectory in human multijoint arm movement. Minimum torque-change model. *Biol Cybern* 61: 89–101, 1989. doi:10.1007/BF00204593.
20. **Harris CM**, **Wolpert DM.** Signal-dependent noise determines motor planning. *Nature* 394: 780–784, 1998. doi:10.1038/29528.
21. **Todorov E**, **Jordan MI.** Optimal feedback control as a theory of motor coordination. *Nat Neurosci* 5: 1226–1235, 2002. doi:10.1038/nn963.
22. **Osu R**, **Kamimura N**, **Iwasaki H**, **Nakano E**, **Harris CM**, **Wada Y**, **Kawato M.** Optimal impedance control for task achievement in the presence of signal-dependent noise. *J Neurophysiol* 92: 1199–1215, 2004. doi:10.1152/jn.00519.2003.
23. **Viviani P**, **Stucchi N.** Biological movements look uniform: evidence of motor-perceptual interactions. *J Exp Psychol Hum Percept Perform* 18: 603–623, 1992. doi:10.1037//0096-1523.18.3.603.
24. **Levit-Binnun N**, **Schechtman E**, **Flash T.** On the similarities between the perception and production of elliptical trajectories. *Exp Brain Res* 172: 533–555, 2006. doi:10.1007/s00221-006-0355-4.
25. **Viviani P**, **Terzuolo C.** Space-time invariance in learned motor skills. *Advance Psychol* 1: 525–533, 1980. doi:10.1016/S0166-4115(08)61967-6.
26. **Huh D**, **Sejnowski TJ.** Spectrum of power laws for curved hand movements. *Proc Natl Acad Sci USA* 112: E3950–E3958, 2015. doi:10.1073/pnas.1510208112.
27. **Polyakov F**, **Stark E**, **Drori R**, **Abeles M**, **Flash T.** Parabolic movement primitives and cortical states: merging optimality with geometric invariance. *Biol Cybern* 100: 159–184, 2009. doi:10.1007/s00422-008-0287-0.
28. **Likova LT.** Learning-based cross-modal plasticity in the human brain: insights from visual deprivation fMRI. In: *Advanced Brain Neuroimaging Topics in Health and Disease-Methods and Applications*, edited by Papageorgiou TD, Christopoulos GI, Smirnakis SM**.** IntechOpen, 2014, vol. 13, p. 327–358. doi:10.5772/58263.
29. **Likova LT.** Temporal evolution of brain reorganization under cross-modal training: insights into the functional architecture of encoding and retrieval networks. *Proc SPIE Int Soc Opt Eng* 9394: 939417, 2015. doi: 10.1117/12.2178069.
30. **Viviani P**, **Schneider R.** A developmental study of the relationship between geometry and kinematics in drawing movements. *J Exp Psychol Hum Percept Perform* 17: 198–218, 1991. doi:10.1037//0096-1523.17.1.198.
31. **Edelman S**, **Flash T.** A model of handwriting. *Biol Cybern* 57: 25–36, 1987. doi:10.1007/BF00318713.
32. **Flash T**, **Sejnowski TJ.** Computational approaches to motor control. *Curr Opin Neurobiol* 11: 655–662, 2001. doi:10.1016/s0959-4388(01)00265-3.
33. **Soechting JF**, **Lacquaniti F**, **Terzuolo CA.** Coordination of arm movements in three-dimensional space. Sensorimotor mapping during drawing movement. *Neurosci* 17: 295–311, 1986. doi:10.1016/0306-4522(86)90248-4.
34. **Lacquaniti F.** Central representations of human limb movement as revealed by studies of drawing and handwriting. *Trends Neurosci* 12: 287–291, 1989. doi:10.1016/0166-2236(89)90008-8.